

# Radii and binding energies in oxygen: a puzzle for nuclear forces

V. Lapoux<sup>1,\*</sup>, V. Somà<sup>1</sup>, C. Barbieri<sup>2</sup>, H. Hergert<sup>3</sup>, J. D. Holt<sup>4</sup>, and S. R. Stroberg<sup>4</sup>  
<sup>1</sup> *CEA, Centre de Saclay, IRFU, Service de Physique Nucléaire, 91191 Gif-sur-Yvette, France*  
<sup>2</sup> *Department of Physics, University of Surrey, Guildford GU2 7XH, United Kingdom*  
<sup>3</sup> *National Superconducting Cyclotron Laboratory and Department of Physics and Astronomy, Michigan State University, East Lansing, MI 48824, USA and*  
<sup>4</sup> *TRIUMF, 4004 Wesbrook Mall, Vancouver, British Columbia, Canada V6T 2A3*

(Dated: December 18, 2015)

We present a systematic study of both nuclear radii and binding energies in (even) oxygen isotopes from the valley of stability to the neutron drip line. A thorough analysis of the available experimental information of oxygen radii is carried out and is compared to state-of-the-art *ab initio* calculations along with binding energy systematics. We show that, in spite of a good reproduction of the latter, *ab initio* calculations with conventional inter-nucleon potentials derived within chiral effective field theory fail to provide a realistic description of charge and matter radii. A novel unconventional version of two- and three-nucleon forces leads to considerable improvement of the simultaneous description of the three observables for stable isotopes, but shows deficiencies for the most neutron-rich systems. Thus, crucial challenges related to the development of nuclear interactions remain.

PACS numbers: 25.60.-t, 21.10.-k, 21.10.Jx, 24.10.Eq

Linking a universal description of atomic nuclei, self-bound mesoscopic systems of  $A$  interacting fermions (with  $A$  ranging from one to a few hundreds), to elementary interactions among their constituents, protons and neutrons, has long been and remains one of the fundamental challenges of nuclear physics. If accomplished, such a link would be beneficial in two aspects: (i) for a deep understanding of known nuclei (both stable, naturally existing on earth and unstable, created in laboratories worldwide) and (ii) to predict on reliable bases the features of the thousands of yet unobserved ones. Many of the latter will not be, in a foreseeable future, experimentally at reach; yet they are crucial e.g. to understand the nucleosynthesis of heavy elements.

Among all possible observables, ground-state characteristics, notably masses (expressed as binding energies) and sizes (expressed as root mean square radii), represent the first quantities that combined experimental and theoretical advances must address. Even these basic properties emerge nontrivially from the complex nucleon dynamics and pose considerable challenges to theoretical approaches. Where total energies tell us about the degree of binding and thus determine the frontiers of the nuclear chart, radii may eventually display exotic behaviour (e.g. the formation neutron distributions that extend well beyond the typical nuclear size, referred to as nuclear halos) and need to be consistently well accounted for.

Experimentally, efforts are devoted to measuring masses and radii along isotopic chains from drip line to drip line, i.e. for all existing isotopes of a given element. In 2015, the neutron drip line is known only up to  $Z=8$  (with  $^{24}\text{O}$ ) where, on the proton-rich side, it is established up to the protactinium chain  $Z = 91$  (with  $^{212}\text{Pa}$ ). While nuclear masses have been measured between the two drip lines for most of light nuclei, for medium-mass and heavy isotopes their values are more and more poorly

determined as we approach neutron-rich limits [1]. Measurements of charge and matter radii along isotope chains are typically more challenging. Charge radii for stable isotopes have been determined in the past by means of electron scattering [2]; in recent years, laser spectroscopy experiments allow extending such measurements to unstable nuclei with lifetimes down to a few milliseconds [3]. Matter radii are determined by scattering with hadronic probes, usually protons or other nuclei, which requires a modelization of the reaction mechanism and a careful analysis of associated uncertainties [4].

Theoretically, the link between nuclear properties and inter-nucleon forces can be suitably investigated via *ab initio* many-body calculations. In recent years the derivation of two- and three-nucleon (2N and 3N) interactions within chiral effective field theory (EFT) has provided a systematic starting point for such an approach, ideally connecting nucleonic systems with the underlying theory of quantum chromodynamics [5, 6]. *Ab initio* techniques have themselves undergone major progress and extended their domain of applicability both in mass [7–9] and in terms of accessible (open-shell) isotopes for a given element [10–17]. As a result, today the structure of light and medium-mass nuclei can be viewed as a testing ground for our basic understanding of nuclear forces.

The heaviest element where a systematic comparison between measured and calculated masses and radii can be performed *from drip line to drip line* is oxygen. Recently, the case of binding energies along the oxygen isotopic chain has been investigated within several microscopic and *ab initio* approaches, establishing the crucial role played by 3N forces in the description of the neutron drip line at  $^{24}\text{O}$  (i.e. in explaining the so-called “oxygen anomaly”) [11, 18–21]. The excellent agreement between experimental data and theoretical calculations based on a next-to-next-to-next-to-leading order

( $N^3$ LO) 2N and  $N^2$ LO 3N chiral interaction (EM) [22–24] was greeted as a milestone for ab initio calculations and modern models of inter-nucleon interactions, even though a consistent description of nuclear radii could not be achieved at the same time. Later on, calculations of heavier systems [7, 8, 12] and infinite nuclear matter [25, 26] have confirmed a systematic underestimation of charge radii, as well as a sizeable overbinding and too spread-out spectra, all consistently pointing to an incorrect reproduction of the saturation properties of nuclear matter. This led to the development of a novel nuclear interaction, labelled  $NNLO_{\text{sat}}$  [27], unconventional in the sense that experimental constraints from C and O isotopes were included in the fit of the coupling constants. Although first applications point to good predictive power [27, 28] for ground-state properties, the performance of the  $NNLO_{\text{sat}}$  potential remains to be tested along isotopic chains and for excited states.

Here we present a systematic study of charge and matter radii as well as binding energies in (even) oxygen isotopes, from the valley of stability to the neutron drip line. In doing so, we first carry out a new analysis of matter radii and then compare to ab initio calculations of these observables. Experimental data on charge ( $r_{ch}$ ) and proton ( $r_p$ ) radii are obtained from elastic electron (e,e) scattering and available only for the stable  $^{16-18}\text{O}$ . (e,e) cross sections allow extracting not only charge rms radii but also analytical forms of fitted experimental charge densities. Standard forms include 2- or 3-parameter Fermi (2pF or 3pF) profiles [29, 30]. Proton ground-state (gs) densities (proton distributions inside the nucleus in its center-of-mass frame) can be deduced from the experimental charge distribution by unfolding [31] the finite size of the charge distribution of the proton (whose rms charge radius is 0.877(7) fm [32]).

Matter ( $r_m$ ) radii values are evaluated via (p,p) scattering for  $^{16,18}\text{O}$  as well as for weakly-bound  $^{20,22}\text{O}$ . In the case of stable nuclei, proton density distributions can be first benchmarked on (e,e) cross sections and subsequently inserted in optical model potential (OMP) calculations. By adjusting on (p,p) scattering data, neutron densities and hence matter radii can be deduced. This was done e.g. for  $^{16}\text{O}$  in Ref. [33], where data sets for angular distributions of (p,p) and (n,n) at incident nucleon energies between 15 and 40 MeV were reproduced using the “experimental” matter density [31] deduced from electron scattering [29]. Such a density is obtained assuming a similar form of the 2pF function for proton and neutron densities. For data set with errors of less than 10 %, it is possible to discriminate between various neutron profiles, which translates into an uncertainty of  $\pm 0.1$  fm for matter radii. A similar extraction for neutron and matter densities was done for  $^{18}\text{O}$ . In the following discussion, we refer to these densities as the experimental (“exp”) densities.

The energy- and density-dependent JLM potential [36],

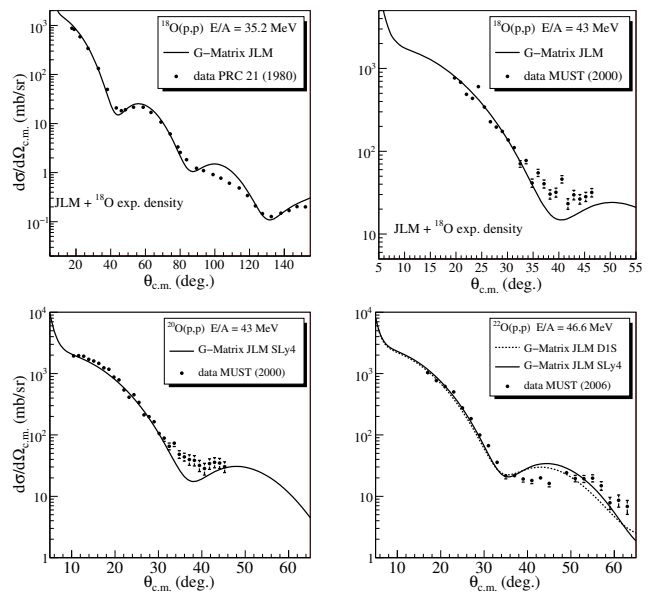


FIG. 1. Experimental elastic cross sections compared to OMP calculations. (Top) Case of  $^{18}\text{O}(p,p)$  for two different incident energies [34, 35]. (Bottom) Cases of  $^{20,22}\text{O}(p,p)$  [35].

derived from the G-matrix formalism, has been extensively used in the analysis of nucleon scattering data for a wide range of nuclei. This complex potential depends only on the incident energy  $E$  and on neutron and proton densities. Here we use the standard form  $U_{JLM}(\rho, E)(r) = \lambda_V V(\rho, E)(r) + i\lambda_W W(\rho, E)(r)$ , with  $\lambda_V = \lambda_W = 1$ . We first performed OMP calculations for  $^{18}\text{O}$  with “exp” input densities and compare them to data collected at 35.2 A-MeV in direct kinematics [34], and at 43 A-MeV in inverse kinematics [35]. As shown in Fig. 1 (upper panels), calculations are in good agreement with (p,p) data, which confirms the validity of the OMP approach provided that realistic densities are employed. The associated matter radius is  $r_m = 2.7$  fm. We repeated the analysis using microscopic densities generated by Hartree-Fock BCS calculations [35] with the effective Skyrme Sly4 [37] interaction. Results are very similar to the ones of Fig. 1, with a corresponding value for the matter radius of  $r_m = 2.7 \pm 0.1$  fm, which coincides with the one from “exp” densities. This validates the use of OMP calculations together with microscopic densities to estimate matter radii from (p,p) cross sections [4].

For  $^{20,22}\text{O}$ , elastic proton scattering cross sections were measured using oxygen beams in inverse kinematics at 43 and 46.6 A-MeV respectively [35, 38]. We extended our OMP calculations with microscopic densities to compute these (p,p) cross sections. Results are shown in Fig. 1 (lower panels). In order to test the sensibility to the details of the microscopic input, we compare for  $^{22}\text{O}$  results with those obtained with densities from Hartree-Fock-

Bogoliubov calculations based on the effective Gogny force D1S [39, 40]. Similar calculations are extensively described in Ref. [41] for the case of  $^{16}\text{O}(\text{p,p})$ . In both cases, and for both microscopic densities for  $^{22}\text{O}$ , (p,p) cross sections are well reproduced. Resulting matter radii are  $r_m = 2.90$  fm in  $^{20}\text{O}$  along with  $r_m = 2.96$  and  $3.03$  fm in  $^{22}\text{O}$  for Sly4 and D1S densities, respectively. In particular, an overall satisfactory agreement is obtained for the description of  $^{22}\text{O}(\text{p,p})$  data, showing that  $r_m$  radii associated to these input densities are, within  $\pm 0.1$  fm, realistic to account for the interaction processes. The experimental values obtained through the (p,p) analysis are summarised in Tab. I.

Another way of deducing matter radii is provided by studying interaction cross sections ( $\sigma_I$ ) [42]. In Fig. 2, we compare the complete set of experimental matter radii for  $^{16,18,20,22}\text{O}$  from (e,e) and (p,p) scattering to values obtained from  $\sigma_I$  measurements, reported in Ref. [42] and Ref. [43] with a new analysis for  $^{22,23}\text{O}$  (see also Tab. I). We notice that radii from the two analyses are inconsistent. Matter radii from  $\sigma_I$  are usually extracted without including correlations in the target, which may influence scattering amplitudes. Our analysis of (e,e) and (p,p) providing matter radii with an uncertainty of the order of 0.1 fm, we conclude that uncertainties deduced from  $\sigma_I$  are underestimated. This is reinforced by the fact that matter radii of stable isotopes from electron scattering are also underestimated. Consequently, we focus on results obtained from (e,e) and (p,p) cross sections for the comparison with ab initio many-body calculations below.

Two different ab initio many-body approaches are employed, self-consistent Green’s function (SCGF) and in-medium similarity renormalisation group (IM-SRG). Each of them is available in two versions. The first is based on standard expansion schemes and thus applicable only to closed-shell nuclei. It is referred to as Dyson-SCGF (DGF) [44] and single-reference IM-SRG (SR-IM-SRG) [45] respectively. The second version builds on Bogoliubov-type reference states and thus allow for a proper treatment of pairing correlations, resulting in the description of systems displaying an open-shell character. Such version is labelled Gorkov-SCGF (GGF) [10, 46]

A	16	17	18	20	22
$r_{ch}$ (e,e)	2.730 (25)	2.72 (5)	2.75 (5)		
$r_p$	2.59 (7)	2.60 (8)	2.68 (10)		
$r_m$ ( $\sigma_I$ )	2.54 (2)	2.59 (5)	2.61 (8)	2.69(3)	2.88(6)
$r_m$ (p,p)	2.60 (8)	2.67 (10)	2.77 (10)	2.9 (1)	3.0 (1)

TABLE I. Experimental rms radii of oxygen isotopes: charge  $r_{ch}$  and proton  $r_p$  estimated from electron scattering [29, 30] (for  $A = 16, 17, 18$ ); matter  $r_m$  from reaction cross sections  $\sigma_I$  [42];  $r_m$  deduced from heavy-ion [31] and proton [33] scattering data for  $A = 16$ ;  $r_m$  evaluated from proton scattering data (*this work*) for  $A = 18-22$ .

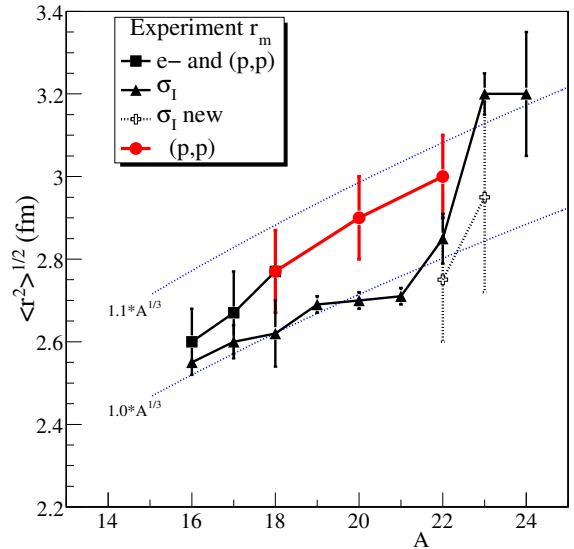


FIG. 2. Experimental values for the  $r_m$  radii, deduced from  $\sigma_I$ , (e,e) and (p,p) measurements (see Tab. I for details). Lines showing an  $A^{1/3}$  behaviour, as predicted from the liquid drop model, are plotted.

and multi-reference IM-SRG (MR-IM-SRG) [11] respectively. Having different ab initio approaches at hand is crucial to benchmark theoretical results and infer as unbiased as possible information on the input of such calculations, i.e. inter-nucleon forces. Moreover, while DGF, SR- and MR-IM-SRG feature a comparable content in terms of many-body expansion, GGF includes a lower amount of many-body correlations, which allows testing the many-body convergence [12].

Calculations have been performed using two sets of 2N and 3N interactions, both constructed within the context of chiral EFT, although following different strategies. The first potential, here labelled EM, includes contributions up to  $N^3\text{LO}$  in the 2N sector [22] and  $N^2\text{LO}$  in the 3N sector [23, 24]. Its coupling constants are fixed uniquely in few-body systems (with  $A \leq 4$ ). In the present work, it is further evolved to a low-momentum scale  $\lambda = 1.88 - 2.0 \text{ fm}^{-1}$  by means of SRG techniques [47]. EM potential represents a standard for ab initio nuclear theory in the sense that it has been widely employed in nuclear structure calculations over the last few years. The second interaction [27], here labelled  $\text{NNLO}_{\text{sat}}$ , was developed very recently and, apart from including contributions only up to  $N^2\text{LO}$  in the chiral EFT expansion (both in 2N and 3N sector), differs from EM in two main aspects. First, the optimisation of the (“low-energy”) coupling constants is performed simultaneously for 2N and 3N terms, i.e. more consistently than for EM. Second, constraints from light nuclei (namely energies and charge radii in some C and O isotopes) are included in the fit of such low-energy con-

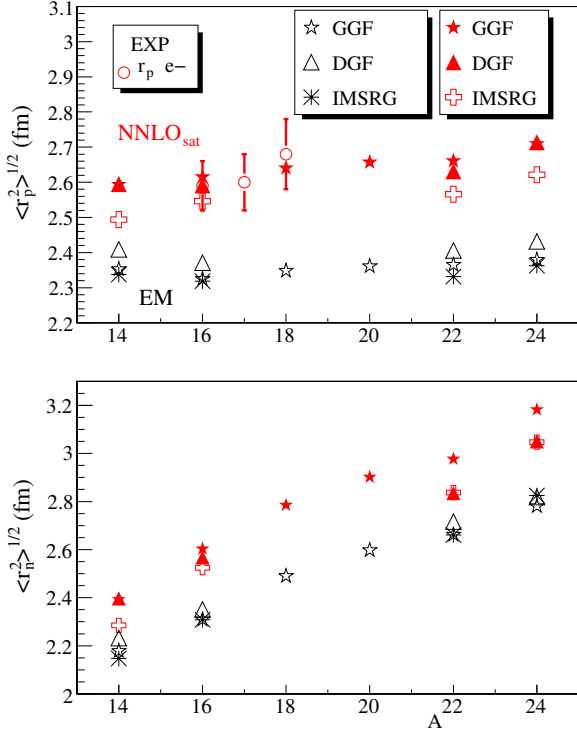


FIG. 3. Rms point-proton (top) and point-neutron (bottom) radii obtained from IM-SRG and SCGF calculations with EM [22–24] and NNLO<sub>sat</sub> [27] input 2N and 3N interactions. In the proton case experimental values from electron scattering [29, 30] are reported.

stants in addition to observables from few-body systems. This second aspect thus represents a departure from the standard ab initio strategy in which parameters in the  $A$ -body sector are fixed uniquely by observables in  $A$ -body systems.

We start by analysing calculations for point-proton and point-neutron radii obtained within the four ab initio schemes with either EM or NNLO<sub>sat</sub> input interactions. Results are displayed in the two panels of Fig. 3, where we compare to experimental values obtained from measured  $r_{ch}$  via

$$\langle r_p^2 \rangle = \langle r_{ch}^2 \rangle - \langle r_p^2 \rangle - \frac{N}{Z} \langle r_n^2 \rangle - r_{DF}^2 - \langle r_{so}^2 \rangle, \quad (1)$$

where  $\langle r_p^2 \rangle$  and  $\langle r_n^2 \rangle$  are the mean-square charge radii of proton and neutron [32],  $r_{DF}^2$  is the Darwin-Foldy relativistic correction [48] and  $\langle r_{so}^2 \rangle$  a charge-density correction originating from nuclear spin-orbit interaction. First, we notice that there is good agreement between the various ab initio calculations, which span 0.05 (0.1) fm when the EM (NNLO<sub>sat</sub>) interaction is used. This gives a measure of the uncertainty on rms radii coming from the approximated solution of the many-body Schrödinger equation, showing that different state-of-the-art schemes achieve a consistent description of this gs observable. In

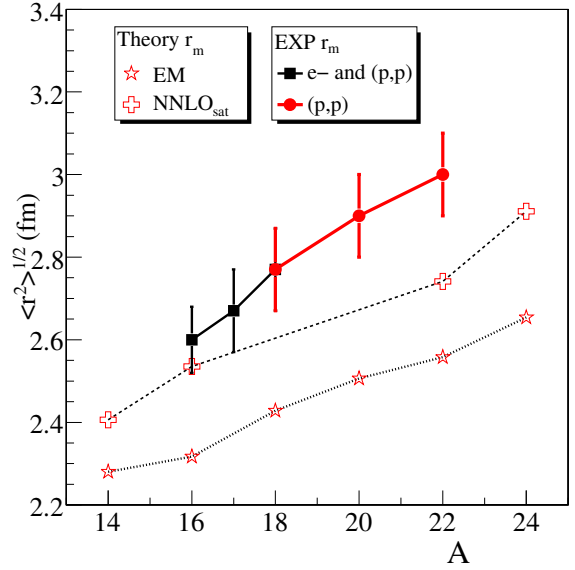


FIG. 4. Matter radii from [29, 30] and our analysis compared to IMSRG ab initio calculations with EM [22–24] and NNLO<sub>sat</sub> [27] input 2N and 3N interactions.

turn, this allows to draw conclusions about the input Hamiltonian. Clear discrepancies are observed between radii computed with EM and NNLO<sub>sat</sub>, with the former being systematically smaller by 0.2-0.3 fm and largely underestimating existing data.

A similar conclusion is drawn from Fig. 4, where evaluated matter radii are compared with IMSRG results. First, rms radii computed with EM underestimate evaluated data by about 0.3-0.4 fm for all isotopes, largely outside experimental uncertainties. Results improve when NNLO<sub>sat</sub> is employed, notably displaying a good agreement with experiment for stable <sup>16</sup>O. Nevertheless, the description deteriorates when moving towards the neutron drip line, with a discrepancy of about 0.2 fm in <sup>22</sup>O.

Finally, in Fig. 5 we compare experimental and calculated total binding energies for isotopes  $A = 14 - 24$ . Here, contrarily to radii, EM and NNLO<sub>sat</sub> interactions yield very similar results, following the trend of available data along the chain both in absolute and in relative terms. A wider span (relative to the use of the different interactions) is observed for GGF calculations. This is presumably due to the fewer many-body correlations resummmed in the second-order GGF scheme with respect to IM-SRG implementations, which play a more important role for the “harder” (in terms of the characteristic scale) NNLO<sub>sat</sub> interaction.

From a general viewpoint, these results reinforce the progress of nuclear ab initio calculations, which nowadays are able to address systematics of isotopic chains beyond light systems and thus provide us with critical feedback on the long-term task of developing elementary inter-nucleon interactions, all in all contributing to

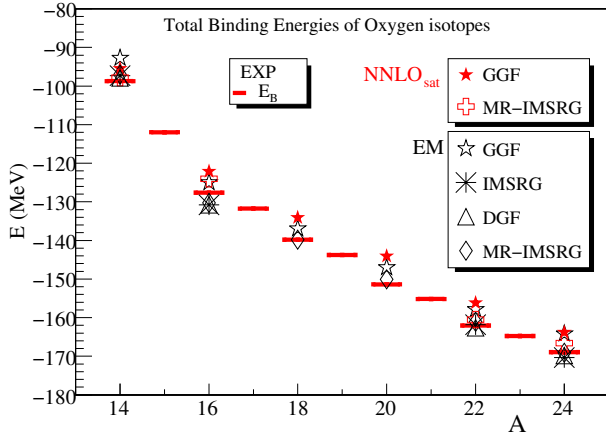


FIG. 5. Experimental binding energies and results from SCGF and IMSRG calculations performed with EM [22–24] and  $\text{NNLO}_{\text{sat}}$  [27] input 2N and 3N interactions.

our basic understanding of atomic nuclei. To this extent, joint theory-experiment and theory-theory analyses are essential and have necessarily to start with a realistic description of both sizes and masses. In this work we focused on the oxygen chain, the heaviest one for which experimental information on both binding energies and radii is available up to the neutron drip line. We showed that analysing (p,p) scattering data allows one to obtain information on nuclear sizes of unstable isotopes within 0.1 fm. The combined comparison of measured charge/matter radii and binding energies with state-of-the-art ab initio calculations offers unique insight on input nuclear forces. On the one hand EM, a current standard for nuclear theory employing only 2-, 3- and 4-body observables in the fit of the low-energy constants thus sticking to the (strict) ab initio strategy, yields an excellent reproduction of binding energies but significantly underestimates charge and matter radii. On the other hand unconventional  $\text{NNLO}_{\text{sat}}$ , while maintaining a good energy systematics, clearly improves the description of radii, though leaving room for refinement for what concerns isotope shifts. Given the alternative fitting procedure (in particular the use of  $r_{ch}$  of  $^{16}\text{O}$  as a constraint), such an output raises questions about the choice of observables that should be included in the fit and the resulting predictive power whenever this strategy is followed.

More precise information on oxygen radii, e.g. via laser spectroscopy measurements, would allow confirming our (p,p) analysis and further refining the present discussion. Future, similar studies in heavier isotopes will also precisely contribute to the systematic development of nuclear forces. From the many-body point of view, the consistent inclusion of higher-body terms in the radius operator is envisaged and might eventually affect conclusions on the radius puzzle. Finally, we stress that a simultane-

ous reproduction of binding energies and radii in stable and neutron-rich nuclei is mandatory for reliable structure but even more for reaction calculations. Scattering amplitudes and nucleon-nucleus interactions evolve as a function of the size, which should be consistently taken into account specially when more microscopic reaction approaches are considered.

The *Espace de Structure et de réactions Nucléaires Théorique* ESNT (<http://esnt.cea.fr>) framework at CEA is gratefully acknowledged for supporting the project that initiated the present work. The authors would like to thank T. Duguet for useful discussions. V.S. and C.B. thank P. Navrátil for providing the interaction matrix elements used in the present SCGF calculations. GGF calculations were performed by using HPC resources from GENCI-TGCC (Contract No. 2015-057392).

\* E-mail address: vlapoux@cea.fr

- [1] G. Audi, M. Wang, A. H. Wapstra, F. G. Kondev, M. MacCormick, X. Xu, and B. Pfeiffer, *Chinese Phys. C* **36**, 1287 (2012).
- [2] R. Hofstadter, *Rev. Mod. Phys.* **28**, 214 (1956).
- [3] J. Billowes and P. Campbell, *J. Phys. G: Nucl. Part. Phys.* **21**, 707 (1995).
- [4] V. Lapoux and N. Alamanos, *Eur. Phys. J. A* **51**, 91 (2015).
- [5] E. Epelbaum, H.-W. Hammer, and U.-G. Meißner, *Rev. Mod. Phys.* **81**, 1773 (2009).
- [6] R. Machleidt and D. Entem, *Phys. Rep.* **503**, 1 (2011).
- [7] H. Hergert, S. K. Bogner, S. Binder, A. Calci, J. Langhammer, R. Roth, and A. Schwenk, *Phys. Rev. C* **87**, 034307 (2013).
- [8] S. Binder, J. Langhammer, A. Calci, and R. Roth, *Phys. Lett. B* **736**, 119 (2014).
- [9] G. Hagen, T. Papenbrock, M. Hjorth-Jensen, and D. J. Dean, *Rep. Prog. Phys.* **77**, 096302 (2014).
- [10] V. Somà, T. Duguet, and C. Barbieri, *Phys. Rev. C* **84**, 064317 (2011).
- [11] H. Hergert, S. Binder, A. Calci, J. Langhammer, and R. Roth, *Phys. Rev. Lett.* **110**, 242501 (2013).
- [12] V. Somà, A. Cipollone, C. Barbieri, P. Navrátil, and T. Duguet, *Phys. Rev. C* **89**, 061301 (2014).
- [13] S. K. Bogner, H. Hergert, J. D. Holt, A. Schwenk, S. Binder, A. Calci, J. Langhammer, and R. Roth, *Phys. Rev. Lett.* **113**, 142501 (2014).
- [14] G. R. Jansen, J. Engel, G. Hagen, P. Navrátil, and A. Signoracci, *Phys. Rev. Lett.* **113**, 142502 (2014).
- [15] A. Signoracci, T. Duguet, G. Hagen, and G. R. Jansen, *Phys. Rev. C* **91**, 064320 (2015).
- [16] T. Duguet, *J. Phys. G: Nucl. Part. Phys.* **42**, 025107 (2015).
- [17] T. Duguet and A. Signoracci, (2015), arXiv:1512.02878 [nucl-th].
- [18] T. Otsuka, T. Suzuki, J. D. Holt, A. Schwenk, and Y. Akaishi, *Phys. Rev. Lett.* **105**, 032501 (2010).
- [19] G. Hagen, M. Hjorth-Jensen, G. R. Jansen, R. Machleidt, and T. Papenbrock, *Phys. Rev. Lett.* **108**, 242501 (2012).
- [20] A. Cipollone, C. Barbieri, and P. Navrátil, *Phys. Rev.*

- Lett. **111**, 062501 (2013).
- [21] K. Hebeler, J. D. Holt, J. Menéndez, and A. Schwenk, *Annu. Rev. Nucl. Part. Sci.* **65**, 457 (2015).
- [22] D. R. Entem and R. Machleidt, *Phys. Rev. C* **68**, 041001 (2003).
- [23] P. Navrátil, *Few-Body Systems* **41**, 117 (2007).
- [24] R. Roth, S. Binder, K. Vobig, A. Calci, J. Langhammer, and P. Navrátil, *Phys. Rev. Lett.* **109**, 052501 (2012).
- [25] A. Carbone, A. Polls, and A. Rios, *Phys. Rev. C* **88**, 044302 (2013).
- [26] G. Hagen, T. Papenbrock, A. Ekström, K. A. Wendt, G. Baardsen, S. Gandolfi, M. Hjorth-Jensen, and C. J. Horowitz, *Phys. Rev. C* **89**, 014319 (2014).
- [27] A. Ekström, G. R. Jansen, K. A. Wendt, G. Hagen, T. Papenbrock, B. D. Carlsson, C. Forssén, M. Hjorth-Jensen, P. Navrátil, and W. Nazarewicz, *Phys. Rev. C* **91**, 051301 (2015).
- [28] G. Hagen *et al.*, (2015), 10.1038/nphys3529, arXiv:1509.07169 [nucl-th].
- [29] I. Sick and J. S. McCarthy, *Nucl. Phys. A* **150**, 631 (1970).
- [30] H. De Vries, C. W. De Jager, and C. De Vries, *At. Data Nucl. Data Tables* **36**, 495 (1987).
- [31] G. R. Satchler and W. G. Love, *Phys. Rept.* **55**, 183 (1979).
- [32] K. Nakamura *et al.* (Particle Data Group), *J. Phys.* **G37**, 075021 (2010).
- [33] J. S. Petler, M. S. Islam, R. W. Finlay, and F. S. Dietrich, *Phys. Rev. C* **32**, 673 (1985).
- [34] E. Fabrici, S. Micheletti, M. Pignanelli, F. G. Resmini, R. De Leo, G. D’Erasmus, and A. Pantaleo, *Phys. Rev. C* **21**, 844 (1980).
- [35] E. Khan, Y. Blumenfeld, N. V. Giai, T. Suomijärvi, N. Alamanos, F. Auger, G. Colò, N. Frascaria, A. Gillibert, T. Glasmacher, M. Godwin, K. Kemper, V. Lapoux, I. Lhenry, F. Maréchal, D. Morrissey, A. Musumarra, N. Orr, S. Ottini-Hustache, P. Piattelli, E. Pollacco, P. Roussel-Chomaz, J. Roynette, D. Santonocito, J. Sauvestre, J. Scarpaci, and C. Volpe, *Physics Letters B* **490**, 45 (2000).
- [36] J.-P. Jeukenne, A. Lejeune, and C. Mahaux, *Phys. Rev. C* **16**, 80 (1977).
- [37] E. Chabanat, P. Bonche, P. Haensel, J. Meyer, and R. Schaeffer, *Nuclear Physics A* **635**, 231 (1998).
- [38] E. Becheva, Y. Blumenfeld, E. Khan, D. Beaumel, J. M. Daugas, F. Delaunay, C.-E. Demonchy, A. Drouart, M. Fallot, A. Gillibert, L. Giot, M. Grasso, N. Keeley, K. W. Kemper, D. T. Khoa, V. Lapoux, V. Lima, A. Musumarra, L. Nalpas, E. C. Pollacco, O. Roig, P. Roussel-Chomaz, J. E. Sauvestre, J. A. Scarpaci, F. Skaza, and H. S. Than, *Phys. Rev. Lett.* **96**, 012501 (2006).
- [39] J. Dechargé and D. Gogny, *Phys. Rev. C* **21**, 1568 (1980).
- [40] J.-F. Berger, M. Girod, and G. Gogny, *Comput. Phys. Commun.* **63**, 365 (1991).
- [41] M. Dupuis, S. Karataglidis, E. Bauge, J. P. Delaroche, and D. Gogny, *Phys. Rev. C* **73**, 014605 (2006).
- [42] A. Ozawa, T. Suzuki, and I. Tanihata, *Nuclear Physics A* **693**, 32 (2001).
- [43] R. Kanungo *et al.*, *Phys. Rev. C* **84**, 061304 (2011).
- [44] W. H. Dickhoff and C. Barbieri, *Prog. Part. Nucl. Phys.* **52**, 377 (2004).
- [45] K. Tsukiyama, S. Bogner, and A. Schwenk, *Phys. Rev. Lett.* **106**, 222502 (2011).
- [46] V. Somà, C. Barbieri, and T. Duguet, *Phys. Rev. C* **89**, 024323 (2014).
- [47] S. K. Bogner, R. J. Furnstahl, and A. Schwenk, *Prog. Part. Nucl. Phys.* **65**, 94 (2010).
- [48] J. L. Friar, J. Martorell, and D. W. L. Sprung, *Phys. Rev. A* **56**, 4579 (1997).